

2.8, and for understory it was 3.1; the difference is not significant. At BCI, the medians were 2.9 and 4.2, and the difference is significant.

25. The median Ω_{0-10} for wind- or explosively dispersed species at BCI was 4.5; for animal-dispersed species it was 3.0, but the difference was not significant.

26. At Pasoh, the 24 dipterocarp species with $N \geq 50$ individuals had a median Ω_{0-10} of 5.1, compared with 2.8 for all other species. At Lambir, 65 dipterocarps had $\Omega_{0-10} = 21.8$; for other species, $\Omega_{0-10} = 5.3$. Both differences are significant. At Sinharaja, 12 dipterocarps were slightly but not significantly more aggregated than nondipterocarps. HKK and Mudumalai had just three and one dipterocarp species, respectively.

27. C. Wills and R. Condit, *Proc. R. Soc. London Ser. B* **266**, 1445 (1999).

28. K. E. Harms *et al.*, *Nature* **404**, 493 (2000).

29. H. M. Hastings and G. Sugihara, *Fractals: A User's Guide for the Natural Sciences* (Oxford Univ. Press, Oxford, 1993).

30. T. R. Croat, *Flora of Barro Colorado Island* (Stanford Univ. Press, Stanford, CA, 1978).

31. T. C. Whitmore, Ed., *Tree Flora of Malaya: A Manual for Foresters* (Longman, London, 1972).

32. N. Manokaran *et al.*, *Stand Table and Distribution of Species in the 50-ha Research Plot at Pasoh Forest Reserve*, Research Data (Forest Research Institute of Malaysia, Kepong, Malaysia, 1992), vol. 1.

33. R. Condit, *Tropical Forest Census Plots* (Springer-

Vergal and R. G. Landes Co., Berlin, and Georgetown, TX, 1998).

34. Supported by the Indian Institute of Science, the University of Peradeniya (Sri Lanka), the Sarawak Forest Department (Malaysia), the Forest Research Institute of Malaysia, the Royal Thai Forest Department, the Smithsonian Tropical Research Institute, the Japanese National Institute of Environmental Studies, the Japanese Ministry of Education and Science, the National Science Foundation, and the John D. and Catherine T. MacArthur Foundation. R.C. thanks J. Franklin's group in the College of Forest Resources at the University of Washington for support during a sabbatical.

23 December 1999; accepted 28 March 2000

Mechanism of ATP-Dependent Promoter Melting by Transcription Factor IIH

Tae-Kyung Kim,¹ Richard H. Ebright,² Danny Reinberg^{1*}

We show that transcription factor IIH ERCC3 subunit, the DNA helicase responsible for adenosine triphosphate (ATP)-dependent promoter melting during transcription initiation, does not interact with the promoter region that undergoes melting but instead interacts with DNA downstream of this region. We show further that promoter melting does not change protein-DNA interactions upstream of the region that undergoes melting but does change interactions within and downstream of this region. Our results rule out the proposal that IIH functions in promoter melting through a conventional DNA-helicase mechanism. We propose that IIH functions as a molecular wrench: rotating downstream DNA relative to fixed upstream protein-DNA interactions, thereby generating torque on, and melting, the intervening DNA.

Human transcription factor IIH consists of nine polypeptides with masses of 31 to 90 kD (1-3). IIH is responsible for three critical functions in transcription: phosphorylation of the COOH-terminal domain (CTD) of the RPB1 subunit of RNA polymerase II (RNAPII), promoter melting, and promoter clearance.

IIH-dependent CTD phosphorylation re-

quires ATP and is mediated by the IIH cdk7 subunit, which is a cyclin-dependent protein kinase (1-3). The role of IIH in promoter melting is to melt about one turn of DNA encompassing the transcription start site to yield the "transcription bubble" (4, 5). This process requires ATP (4, 5) and is mediated by the IIH ERCC3 subunit (6, 7) (also referred to as

XPB), which, in isolation, exhibits 3'-5' DNA-helicase activity (6, 8, 9). The role of IIH in promoter clearance is to stimulate escape of transcription elongation complexes stalled at positions +10 to +17 (10-12). Like promoter melting, promoter escape requires ATP (10-13) and is mediated by the IIH ERCC3 subunit (14).

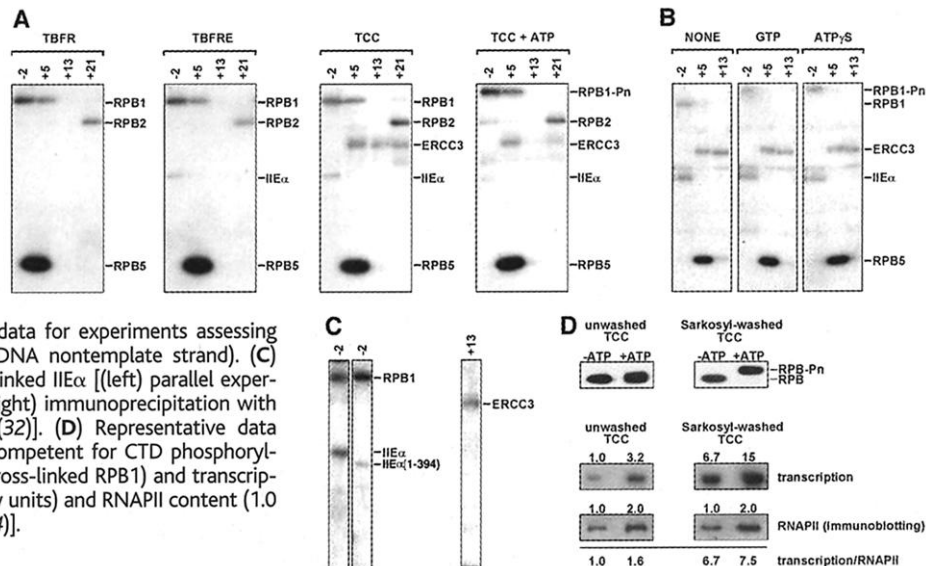
The fact that promoter melting involves generation of single-stranded DNA (ssDNA) and that promoter escape involves a species containing ssDNA, together with the fact that the IIH subunit that mediates these processes exhibits DNA-helicase activity, has led to the proposal that IIH functions in these processes through a conventional DNA-helicase mechanism, with direct interactions between IIH and ssDNA (1-3, 15). However, no direct evidence has been obtained in support of this proposal.

As a first step to understand the mechanism

¹Howard Hughes Medical Institute, Division of Nuclear Acids Enzymology, Department of Biochemistry, University of Medicine and Dentistry of New Jersey, Robert Wood Johnson Medical School, Piscataway, NJ 08854, USA. ²Howard Hughes Medical Institute, Waksman Institute, and Department of Chemistry, Rutgers University, Piscataway, NJ 08854, USA

*To whom correspondence should be addressed. E-mail: reinbedf@umdnj.edu

Fig. 1. Results of protein-DNA photo-cross-linking experiments. **(A)** Representative data. TBFR, transcription-complex intermediate containing RNAPII, TBP, IIB, IIF, and promoter DNA (18); TBFRE, TBFR plus IIE; TCC, transcriptionally competent complex, consisting of TBFR plus IIE and IIH; TCC + ATP, transcriptionally competent complex after ATP-dependent CTD phosphorylation and promoter melting. RPB1 and RPB1-Pn denote forms of the largest subunit of RNAPII having unphosphorylated CTD and phosphorylated CTD, respectively. Data are shown for positions -2, +5, +13, and +21 of the DNA nontemplate strand. **(B)** Representative data for experiments assessing NTP specificity (positions -2, +5, and +13 of DNA nontemplate strand). **(C)** Representative data confirming identities of cross-linked IIE α [(left) parallel experiment with IIE α (1-394) (37, 49)] and IIH ERCC3 [(right) immunoprecipitation with antibody to ERCC3 of cross-linked polypeptide (32)]. **(D)** Representative data demonstrating increase in fraction of complexes competent for CTD phosphorylation (top); analysis of electrophoretic mobility of cross-linked RPB1 and transcription [bottom; quantitation of transcription (arbitrary units) and RNAPII content (1.0 unit = 20 fmol RNAPII) upon Sarkosyl washing (24)].



of action of IIH in promoter melting and promoter escape, we have used systematic site-specific protein-DNA photo-cross-linking (16–18) to define the location of IIH relative to promoter DNA in transcription initiation complexes. In published work, we have used site-specific protein-DNA photo-cross-linking to analyze a transcription-complex intermediate containing human RNAPII, TATA-binding protein (TBP), transcription factor IIB, transcription factor IIF, and promoter DNA (18). In this report, we extended this analysis to the complex that also contains human transcription factors IIE and IIH (19). This latter complex contains 27 distinct polypeptides, has a molecular mass of ~2 MD, and is the minimal complex generally sufficient for transcription initiation (transcriptionally competent complex, TCC) (1).

Pilot experiments indicated that formation of the TCC was accompanied by substantial formation of nonproductive and nonspecific complexes, with only a small minority (~5%) of complexes being competent for CTD phosphorylation and transcription (Fig. 1D). To eliminate complications due to formation of nonproductive and nonspecific complexes, we formed complexes on immobilized promoter DNA fragments (20, 21), washed immobilized complexes with Sarkosyl to remove nonproductive and nonspecific complexes (21–23), and performed cross-linking by ultraviolet (UV) irradiation of immobilized, washed complexes in situ (21). Control experiments established that this procedure results in substantial increases in the proportion of complexes competent for CTD phosphorylation and transcription (Fig. 1D) (24).

We constructed and analyzed 68 site-specifically derivatized DNA fragments, each containing a phenyl-azide photoactivatable cross-linking agent at a single, defined phosphate of the adenovirus major late promoter (positions –43 to +25; Fig. 2) (20, 25). Data for the TCC in the absence of ATP—i.e., under conditions in which the promoter is unmelted (1–5, 26)—are presented in Figs. 1A [representative data, see also (27)] and 2A (summary of data). Together with data for the transcription-complex intermediate analyzed previously (18, 28), the data permit three main conclusions:

1) Entry of IIE and IIH into the complex does not substantially alter protein-DNA interactions by RNAPII, TBP, IIB, and IIF (Fig. 2A, black and blue bars) (18, 28, 29). We conclude that IIE and IIH “slot” into the complex without substantially altering the conformations and interactions of RNAPII, other general transcription factors, and DNA.

2) IIE makes extensive interactions with promoter DNA (Fig. 2A; green bars). Interactions are made both by the IIE β subunit (15, 30) and the IIE α subunit (31). IIE interacts with DNA in and immediately downstream of the transcription-bubble region.

3) IIH makes extensive interactions with promoter DNA (Fig. 2A; red bars). Interactions with the region of the promoter analyzed are made by only one of the nine subunits of IIH: i.e., ERCC3, the subunit that exhibits 3'–5' DNA-helicase activity and that mediates promoter melting and promoter escape (6–9, 14, 32). IIH interacts with DNA exclusively downstream of the transcription-bubble region (positions +3 to at least +25) (33). Interaction of IIH with DNA downstream of the transcription-bubble region is consistent with the observation

that addition of a protein fraction containing IIE and IIH to the RNAPII-TBP-IIB-IIF-promoter complex results in protection of the +20 to +30 region (fraction “CBB”) (34). Projected onto a B form DNA helix, positions at which IIH-DNA cross-linking occurs flank two major grooves and two minor grooves and map to a single face of the DNA helix (27). This face of the DNA helix is offset by 90° and –90° relative to the faces at which cross-linking occurs to the RPB1 and RPB2 subunits of RNAPII (18), consistent with the proposal that

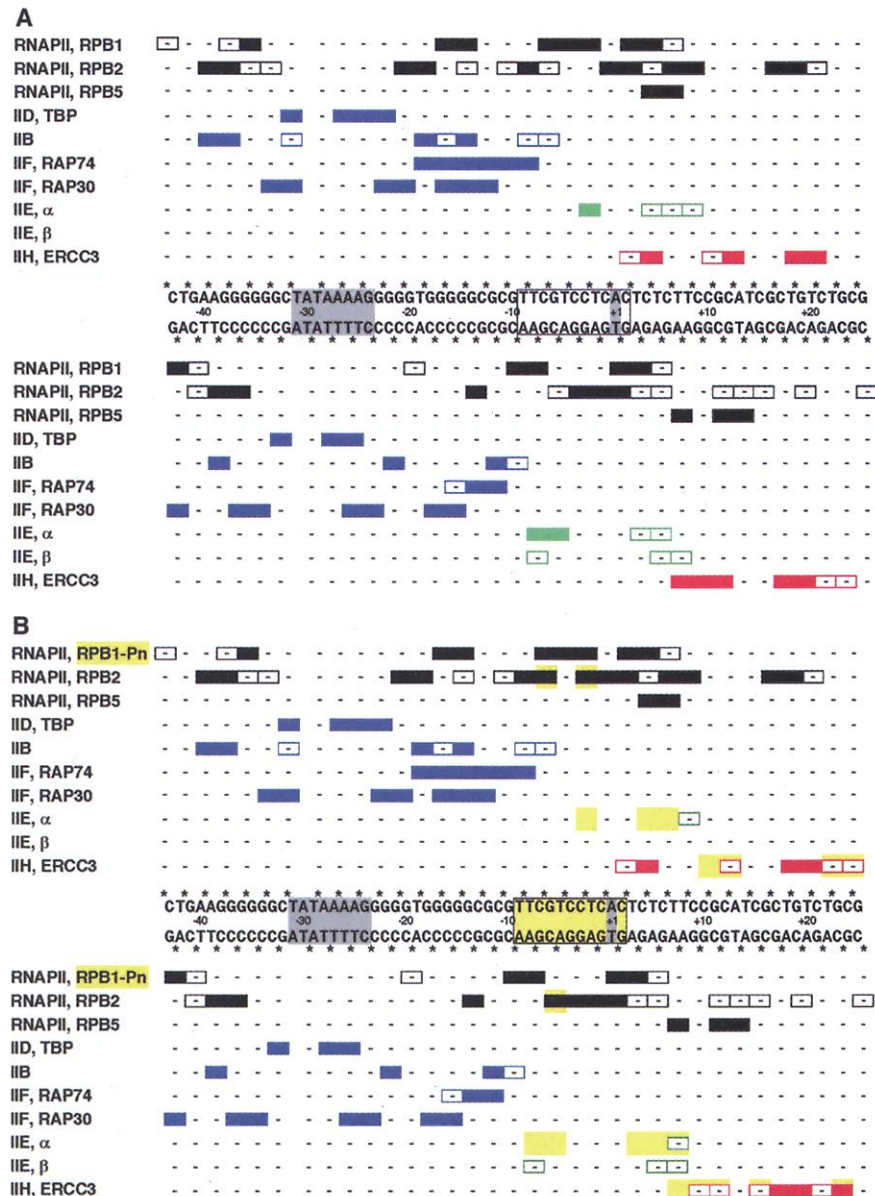


Fig. 2. Summary of photo-cross-linking results (results for nontemplate strand above sequence; results for template strand beneath sequence). Phosphates analyzed are indicated by asterisks. Sites exhibiting cross-linking to RNAPII, TBP/IIB/IIF, IIE, and IIH are indicated by black, blue, green, and red bars, respectively (with sites exhibiting reproducible cross-linking indicated by solid bars and sites exhibiting less reproducible cross-linking indicated by open bars). The TATA element and transcription start are indicated by shading; the transcription-bubble region (positions –9 to +2) (4, 5) is indicated by a rectangle. (A) Results for TCC in the absence of ATP (unphosphorylated CTD, unmelted promoter). (B) Results for TCC in the presence of ATP (phosphorylated CTD, melted promoter), with differences from (A) highlighted in yellow.

IIIH “slots” into the transcription complex, interacting with determinants of DNA not contacted by other components of the complex.

Our finding that IIIH makes no direct interactions with the transcription-bubble region in the TCC in the absence of ATP (Fig. 2A) argues against the proposal that IIIH functions in promoter melting through a conventional DNA-helicase mechanism (which would invoke direct interaction of IIIH with the DNA segment to be melted, in both the double-stranded and single-stranded states). To determine whether IIIH interacts with the transcription-bubble region in the TCC in the presence of ATP—i.e., under conditions in which the transcription bubble is single stranded (1–5, 26)—we carried out a complete parallel cross-linking analysis of the TCC in the presence of ATP (representative data in Fig. 1A; summary of data in Fig. 2B) (27, 35). Comparison of the data for the TCC in the absence and presence of ATP (differences highlighted in yellow in Fig. 2B) permits four main conclusions:

1) Addition of ATP results in apparently quantitative CTD phosphorylation, detected by a decrease in the electrophoretic mobility of cross-linked RPB1 (Fig. 1A and Fig. 2B, yellow).

2) Addition of ATP does not alter protein-DNA interactions upstream of the transcription-bubble region, indicating that ATP does not induce reorganization of the upstream portion of the TCC.

3) Addition of ATP induces changes in protein-DNA interactions in the transcription-bubble region. A new cross-link to the RPB2 subunit of RNAPII appears at position –2 of the nontemplate DNA strand, and quantitative changes in cross-linking to RPB2 and IIE occur on both DNA strands (Figs. 1A and 2B). Parallel experiments with guanosine triphosphate (GTP) and ATP γ S, which support CTD phosphorylation, but not promoter melting (5, 36–39), indicate that these changes are due exclusively to promoter melting (Fig. 1A, fourth panel, and Fig. 1B).

4) Addition of ATP induces changes in IIIH-DNA interactions downstream of the transcription-bubble region. IIIH-DNA interactions are made exclusively by the ERCC3 subunit of IIIH, occur exclusively downstream of the transcription-bubble region, and are made exclusively with double-stranded DNA (dsDNA), as in the absence of ATP (Fig. 2). The positions of IIIH-DNA cross-links map to the same face of the DNA helix as in the absence of ATP (27). However, there are both qualitative and quantitative changes in individual IIIH-DNA cross-links, with, in general, decreased cross-linking in the minor groove centered at position +10 and increased cross-linking in the minor groove centered at +20 (Figs. 1A and 2B) (27). Analysis of nucleotide triphosphate (NTP) specificity indicates that these changes, like those in the transcription-bubble region, are due exclusively to promoter melting (Fig. 1A, fourth panel, and Fig. 1B).

Our results establish that IIIH does not interact with DNA in the transcription-bubble region—neither in the TCC with a double-stranded transcription-bubble region nor in the TCC with a single-stranded transcription-bubble region. Thus, our results rule out, at least for this promoter, the proposal that IIIH functions in promoter melting through a conventional DNA-helicase mechanism.

Our finding that the ERCC3 subunit of IIIH interacts with the DNA segment downstream of the transcription-bubble region, together with our finding that addition of ATP does not alter protein-DNA interactions upstream of the transcription bubble, but does alter protein-DNA interactions in and downstream of the transcription bubble, suggests a specific alternative model for IIIH function in promoter melting (Fig. 3A).

According to the model, in the TCC in the absence of ATP, sequence-specific protein-DNA interactions by TBP (40, 41), IIB (42), and possibly IIF rotationally fix promoter DNA upstream of the transcription-bubble region; the RPB1, RPB2, and RPB5 subunits of RNAPII encompass, but do not rotationally fix, the DNA segment downstream of the transcription-bubble region; and the ERCC3 subunit of IIIH interacts with this same DNA segment, interacting with a face of the DNA helix left accessible by RPB1, RPB2, and RPB5 (Fig. 2A and Fig. 3A, left panel) (27). Upon addition of ATP, ERCC3 rotates the DNA segment downstream of the transcription-bubble region by about one turn relative to the fixed upstream interactions, inducing melting of about one turn of DNA between ERCC3 and the fixed upstream interactions and yielding a single-stranded transcription bubble (Fig. 3A, right panel).

In this model, ERCC3 acts as a molecular “wrench,” interacting with the downstream DNA segment to generate torque that nucleates formation of the transcription bubble, facilitates downstream extension of the transcription bub-

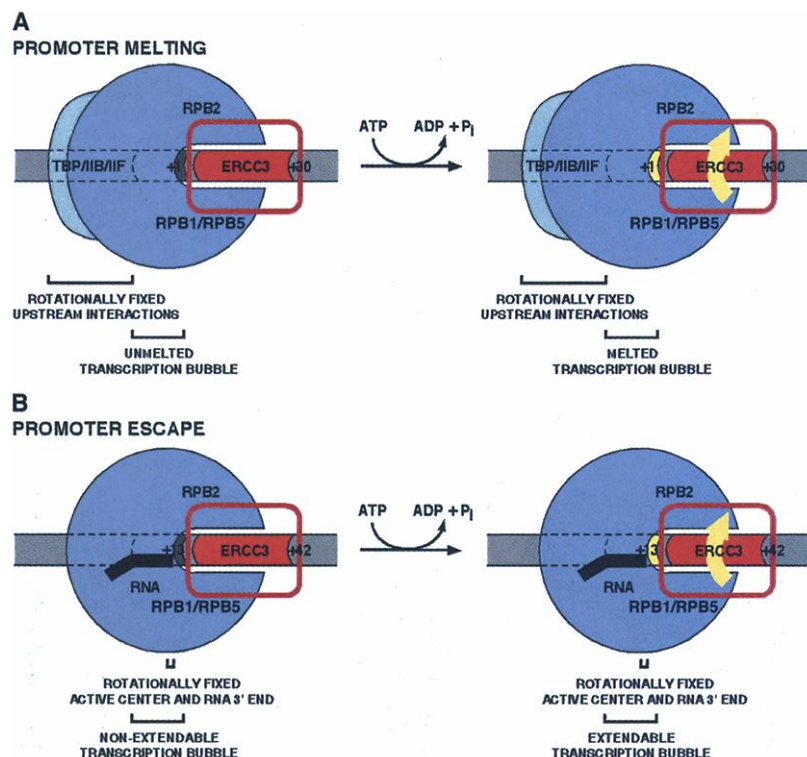


Fig. 3. Models. **(A)** Promoter melting. In the presence of ATP, the IIIH ERCC3 subunit rotates the DNA segment downstream of the transcription-bubble region relative to rotationally fixed upstream interactions, inducing melting of the transcription-bubble region. RNAPII is in dark blue, with the positions of the RNAPII RPB1, RPB2, and RPB5 subunits indicated; TBP, IIB, and IIF are in light blue; and IIIH ERCC3 is indicated by an open red rectangle. Promoter DNA is drawn with upstream DNA at left, transcription-bubble region at center, and downstream DNA at right; the DNA segment contacted by the IIIH ERCC3 is in red. ATP-dependent changes are highlighted in yellow. ADP, adenosine diphosphate; P_i, inorganic phosphate. **(B)** Promoter escape. IIIH function in promoter escape involves stimulating escape by transcription elongation complexes stalled after synthesis of 10 to 17 nt of RNA (10–12). IIIH translocates with RNAPII during synthesis of the first 10 to 17 nt of RNA (23), and thus ERCC3 interacts with the DNA segment downstream of the transcription bubble in the stalled elongation complex [e.g., positions +16 to +42 for an elongation complex stalled at +13 (44); left]. In the presence of ATP, ERCC3 rotates the DNA segment downstream of the transcription bubble relative to the rotationally fixed upstream interactions, facilitating downstream extension of the transcription bubble and/or stabilization of the transcription bubble (right).

ble, and/or stabilizes the transcription bubble. The presence of RPB1, RPB2, and RPB5 on adjacent faces of the downstream DNA segment presumably would preclude ERCC3 from rotating by one full turn in a single step (Fig. 3A, right panel). Therefore, we envision that ERCC3 acts as a "ratchet wrench," effecting rotation by one full turn in multiple smaller increments.

An important aspect of the model is that it suggests a possible common mechanism for IIH function in promoter melting and promoter escape—with IIH functioning in each case by rotating the DNA segment downstream of the transcription bubble relative to rotationally fixed upstream interactions (Fig. 3, A and B). IIH function in promoter escape has been shown to require a DNA segment downstream of the transcription bubble [a DNA segment including the +40 region for a transcription elongation complex stalled after synthesis of 10 to 12 nucleotides (nt) of RNA] (43). We suggest that this DNA segment corresponds to the determinant for binding of ERCC3 (Fig. 3B) (44).

References and Notes

1. G. Orphanides, T. Lagrange, D. Reinberg, *Genes Dev.* **10**, 2657 (1996).
2. D. Reinberg et al., *Cold Spring Harbor Symp. Quant. Biol.* **63**, 83 (1998).
3. F. Coin and J.-M. Egly, *Cold Spring Harbor Symp. Quant. Biol.* **63**, 105 (1998).
4. W. Wang, M. Carey, J. D. Gralla, *Science* **255**, 450 (1992).
5. F. Holstege, U. Fiedler, H. M. T. Timmers, *EMBO J.* **16**, 7468 (1997).
6. S. Guzder, P. Sung, V. Bailly, L. Prakash, S. Prakash, *Nature* **369**, 578 (1994).
7. F. Tirode, D. Busso, F. Coin, J.-M. Egly, *Mol. Cell.* **3**, 87 (1999).
8. L. Schaeffer et al., *Science* **260**, 58 (1993).
9. R. Roy et al., *J. Biol. Chem.* **269**, 9826 (1994).
10. A. Dvir, R. Conaway, J. Conaway, *J. Biol. Chem.* **271**, 23352 (1996).
11. _____, *Proc. Natl. Acad. Sci. U.S.A.* **94**, 9006 (1997).
12. K. Kumar, S. Akoulitchev, D. Reinberg, *Proc. Natl. Acad. Sci. U.S.A.* **95**, 9767 (1998).
13. J. Goodrich and R. Tjian, *Cell* **77**, 145 (1994).
14. R. Moreland et al., *J. Biol. Chem.* **274**, 22127 (1999).
15. F. Robert et al., *Mol. Cell.* **2**, 341 (1998).
16. T. Lagrange et al., *Proc. Natl. Acad. Sci. U.S.A.* **93**, 10620 (1996).
17. T.-K. Kim, T. Lagrange, N. Naryshkin, D. Reinberg, R. Ebright, in *Protein-DNA Interactions: A Practical Approach*, A. Travers and M. Buckle, Eds. (IRL Press, Oxford, in press).
18. T.-K. Kim et al., *Proc. Natl. Acad. Sci. U.S.A.* **94**, 12268 (1997).
19. Recombinant TBP, IIB, IIF, IIE, and purified RNAPII (form "IIA") were prepared as in (45). Affinity-purified IIH was prepared as in (46).
20. Derivatized promoter DNA fragments were prepared as in (18), except that the template was ssDNA of M13mp18-AdMLP-2 or M13mp19-AdMLP-2 [prepared by replacement of the Eco RI-Sph I segments of M13mp18 or M13mp19 dsDNA (Roche) by a polymerase chain reaction-generated 210 base pairs (bp) Eco RI-Sph I DNA fragment containing positions -100 to +100 of the adenovirus major late promoter]; the second primer was 5'-GTTGGGAAGGGCGATCCGTG-3'; and, after primer extension, ligation, and desalting steps, products were digested with Ava II, biotin-end-labeled with DNA polymerase I Klenow fragment (Roche) and biotin-14-deoxyadenosine triphosphate (dATP), biotin-14-deoxycytidine triphosphate (dCTP) (GIBCO-BRL),

- deoxyguanosine triphosphate (dGTP), and thymidine triphosphate (TTP) (Pharmacia), and digested by Pvu I.
21. Derivatized promoter DNA fragments (2 nM; 200 Bq/fmol) were incubated for 1 hour at 25°C with streptavidin-coated paramagnetic beads [Dyna beads M-280; Dymal; washed per manufacturer's instruction and treated by incubation for 5 min at 25°C with protease inhibitor mix (Roche); 20 µg] in 20 µl of 5 mM tris-HCl (pH 7.5), 1.0 M NaCl, and 0.5 mM EDTA. Immobilized derivatized promoter DNA fragments were washed three times with 20 µl of transcription buffer [13 mM Hepes-KOH (pH 7.9), 12 mM tris-HCl, 60 mM KCl, 5 mM MgCl₂, 0.1 mM EDTA, 1 mM dithiothreitol (DTT), 0.1 mM phenylmethylsulfonyl fluoride, 2.6% polyethylene glycol [average molecular weight (MW_{av}) = 8 kD], poly(dC-dC) (MW_{av} = 700 kD; 25 µg/ml), bovine serum albumin (BSA; 50 µg/ml), and 12% glycerol] and were incubated for 40 min at 30°C with 20 µl of transcription buffer containing 7.5 nM human RNAPII, 5 nM TBP, 5 nM IIB, 5 nM IIF, 5 nM IIE, and 6 nM affinity-purified IIH. Resulting immobilized complexes were washed with 20 µl of transcription buffer containing 0.05% Sarkosyl and twice with 20 µl of transcription buffer (30 s at 25°C per wash), were further incubated for 5 min at 25°C in 20 µl of transcription buffer containing 0 or 300 µM ATP, and were UV irradiated [method as in (18)]. Cross-linked polypeptides were identified by performing nuclease digestion, SDS-polyacrylamide gel electrophoresis (SDS-PAGE), and autoradiography [methods as in (18)].
22. D. Hawley and R. Roeder, *J. Biol. Chem.* **260**, 8163 (1985).
23. L. Zawel, K. Kumar, D. Reinberg, *Genes Dev.* **9**, 1479 (1995).
24. Immobilized complexes were prepared as in (21) with 1059-bp biotin-end-labeled DNA fragments containing the adenovirus major late promoter fused to a G-less cassette [prepared by Hind III digestion of pΔ50 (47), biotin end-labeling as in (20), and Ssp I digestion]. The resulting immobilized complexes—without washing (Fig. 1D, left panel) or with washing as in (21) (Fig. 1D, right panel)—were analyzed for CTD phosphorylation [analysis of electrophoretic mobility of cross-linked RPB1; method as in (21)], transcription [incubation for 5 min at 25°C in 20 µl of transcription buffer containing 16 µM [³²P]uridine triphosphate (UTP) (1 Bq/fmol), 500 µM ATP, and 500 µM CTP; addition of UTP to 600 µM and further incubation 30 min at 25°C; and phenol/chloroform extraction, ethanol precipitation, and urea-PAGE analysis of products], and RNAPII content [immunoblottings of serial dilutions with monoclonal antibody to CTD 8WG16 (48)]. The increase in transcription per fmol of RNAPII upon Sarkosyl washing was 5.5 (±0.4)-fold [mean (±SEM) from six determinations].
25. Derivatized DNA fragments containing cross-linking agent at sites within the transcription-bubble region (positions -8, -4, and +1 of nontemplate strand and positions -10, -6, and -2 of template strand) were confirmed to be functional in transcription initiation [method as in (24)].
26. Potassium permanganate footprinting (4, 5) of Sarkosyl-washed, immobilized TCC confirms that the transcription-bubble region is unmelted in the absence of ATP and melted in the presence of ATP (T.-K. Kim, R. H. Ebright, D. Reinberg, data not shown). Sarkosyl-washed, immobilized complexes were prepared as in (21) with 208-bp biotin-end-labeled, ³²P-end-labeled DNA fragments (prepared as in (20)), except that the first primer was nonradioactive; the second primer was 5'-TGACCGGCAGCAAATG-3'; and, after primer extension, ligation, and desalting steps, products were digested with Eco RI, biotin-end-labeled with DNA polymerase I Klenow fragment and biotin-14-dATP, dCTP, dGTP, and TTP, digested with Hind III, and ³²P-end-labeled with DNA polymerase I Klenow fragment and [³²P]dATP, [³²P]dCTP, [³²P]dGTP, and [³²P]TTP and with DTT at 0.5 mM. Footprinting reactions were initiated by addition of 1 µl of 200 mM KMnO₄ and were terminated after 3 min at 25°C by addition of 1 µl of β-mercaptoethanol. Products were extracted with phenol/chloroform, precipitated with ethanol, incubated for 30 min at 90°C in 10% piperidine, precipitated with 1-butanol, washed with 80% ethanol, washed with ethanol, and analyzed by urea-PAGE.

27. Supplemental material is available on Science Online at www.sciencemag.org/feature/data/1047530.shl.
28. Experiments with the TBP-IIB-IIF-RNAPII-promoter complex in (18) were performed with unwashed complexes. Experiments with the TBP-IIB-IIF-RNAPII-promoter complex were repeated with Sarkosyl-washed, immobilized complexes [method as in (27)]. In cases where different results were obtained with unwashed and washed complexes, results for washed complexes were considered definitive.
29. Our results contradict cross-linking results in (15) suggesting major reorganization of the complex upon entry of IIE and IIH. We attribute this difference to the fact that the results in (15) were obtained with unresolved mixtures of TCC, nonspecific complexes, and nonproductive complexes (see Fig. 1D). We performed representative experiments with unwashed TCC; in these experiments, we observed extensive additional cross-linking to IIF and RPB2, reminiscent of results in (15).
30. F. Robert, D. Forget, J. Li, J. Greenblatt, B. Coulombe, *J. Biol. Chem.* **271**, 8517 (1996).
31. Assignments of cross-links to IIEα and IIEβ subunits were confirmed in parallel experiments with a IIE derivative having subunits with altered electrophoretic mobilities: IIEα(1-394) (Fig. 1C) (49).
32. Assignments of cross-links to ERCC3 were confirmed by immunoprecipitation with monoclonal antibodies to ERCC3 (Fig. 1C). Immobilized complexes were prepared, washed, UV-irradiated, and nuclease digested as in (21) (no ATP). Products from five parallel 20-µl reactions were pooled, denatured (addition of 10 µl of 10% SDS and 5% NP40 and boiling for 5 min), immunoprecipitated with antibody to ERCC3 [addition of 900 µl of 50 mM tris-HCl (pH 7.9), 150 mM NaCl, 0.1% SDS, 0.5% NP40; addition of 80 µg of monoclonal antibody 8B6/E8 immobilized on protein A beads (46); incubation for 4 hours at 4°C; and washing three times with 1 ml of the same buffer], and analyzed by SDS-PAGE and autoradiography.
33. The downstream boundary of the DNA segment contacted by ERCC3 has not been defined precisely. Preliminary results suggest that the downstream boundary is near position +30.
34. S. Buratowski, S. Hahn, L. Guarente, P. Sharp, *Cell* **56**, 549 (1989).
35. Similar results were obtained upon incubation with ATP for 2 or 5 min.
36. H. Serizawa, R. Conaway, J. Conaway, *Proc. Natl. Acad. Sci. U.S.A.* **89**, 7476 (1992).
37. H. Lu, L. Zawel, L. Fisher, J.-M. Egly, D. Reinberg, *Nature* **358**, 641 (1992).
38. Y. Jiang and J. Gralla, *J. Biol. Chem.* **270**, 1277 (1995).
39. F. Holstege, P. van der Vliet, H. M. T. Timmers, *EMBO J.* **15**, 1666 (1996).
40. Y. Kim, J. Geiger, S. Hahn, P. Sigler, *Nature* **365**, 512 (1993).
41. J. Kim, D. Nikolov, S. Burley, *Nature* **365**, 520 (1993).
42. T. Lagrange, A. Kapanidis, H. Tang, D. Reinberg, R. Ebright, *Genes Dev.* **12**, 34 (1998).
43. A. Dvir, S. Tan, J. Conaway, R. Conaway, *J. Biol. Chem.* **272**, 28175 (1997).
44. Assuming that the spatial relation between ERCC3 and RNAPII is the same in stalled elongation complexes as in the TCC, ERCC3 would be expected to interact with DNA between positions +13 and ~+39 in an elongation complex stalled after synthesis of 10 nt of RNA and between positions +20 and ~+46 in an elongation complex stalled after synthesis of 17 nt of RNA.
45. E. Malodonado, R. Drapkin, D. Reinberg, *Methods Enzymol.* **274**, 72 (1996).
46. G. LeRoy, R. Drapkin, L. Weis, D. Reinberg, *J. Biol. Chem.* **273**, 7134 (1998).
47. M. Sawadogo and R. Roeder, *Cell* **43**, 165 (1985).
48. N. Thomson, D. Aronson, R. Burgess, *J. Biol. Chem.* **265**, 7069 (1990).
49. Y. Ohkuma, S. Hashimoto, C. Wang, M. Horikoshi, R. Roeder, *Mol. Cell. Biol.* **15**, 4856 (1995).
50. Supported by NIH grants GM53665 to R.H.E. and GM37120 to D.R. and by Howard Hughes Medical Investigatorships to R.H.E. and D.R. The authors dedicate this work to the memory of P. Sigler.

1 December 1999; accepted 10 March 2000